Hindawi
Geofluids
Volume 2023, Article ID 7466248, 21 pages
https://doi.org/10.1155/2023/7466248

Research Article

Effect of Liquid Nitrogen Cooling and Heating on Mechanical Properties and Acoustic Emission Characteristics of Coal

Yuhe Cai,[1] Yi Xue,[1] Faning Dang,[1] Linchao Wang,[1] Xue Li,[1] Shanjie Su,[2] Shengcheng Wang,[2] Xinyu Liang,[3] and Shaowei Zhang[1]

[1]*School of Civil Engineering and Architecture, Xi'an University of Technology, Xi'an 710048, China*
[2]*School of Civil Engineering, Xuzhou University of Technology, Xuzhou 221000, China*
[3]*School of electric, Civil Engineering and Architecture, Shanxi University, Taiyuan 030006, China*

Correspondence should be addressed to Yi Xue; xueyi@xaut.edu.cn

Received 8 March 2023; Revised 5 May 2023; Accepted 15 May 2023; Published 5 June 2023

Academic Editor: Hailing Kong

The instability of rock fractures has been extensively studied in domestic and international research. This paper investigates two coal types from the Jiaozuo area, which were subjected to liquid nitrogen cyclic treatment using Brazil's indirect tensile testing (BITT). The study analyzes the characteristics of acoustic emission (AE) and crack formation during the coal cracking process and evaluates the impact of freeze-thaw treatment with liquid nitrogen cycles on the mechanical properties of coals. The results demonstrate that liquid nitrogen has a significant impact on the formation and development of coal fractures under the Brazil splitting test conditions. As the number of cyclic treatments increases, the maximum load-bearing capacity of coal decreases, indicating a gradual reduction in the effective stress on coal samples. Furthermore, the acoustic emission activity intensity of coal mass during phased loading increases as the number of freeze-thaw cycles of liquid nitrogen increases. Finally, during phased loading of coal specimens, the primary factor is the germination, extension, and failure of tensile cracks, while the secondary factor is the development, extension, and failure of shear cracks. Overall, this study provides valuable insights into the behavior of coals under freeze-thaw cycles of liquid nitrogen treatment and highlights the importance of understanding the characteristics of coal fracture instability.

1. Introduction

Recent years have seen the emergence of geothermal energy and other renewable resources as strategic alternatives to traditional energy sources [1]. While geothermal resources are available for direct utilization, heat pump technology, and geothermal fluids from artificial drilling or hot, dry rock masses, the low natural permeability of hot dry rocks poses a challenge to extracting this energy efficiently. To address this challenge, dry hot rock reservoirs must be transformed into enhanced geothermal systems (EGS), with hydraulic fracturing being the most widely-used EGS technique [2, 3]. However, the large amount of water usage and environmental impact associated with fracturing [4, 5] make it unsuitable for application in water-scarce areas rich in coal resources. A highly effective fracturing medium, liquid nitrogen has multiple advantages over hydraulic fracturing for rock masses. Its use resolves the environmental pollution and reservoir damage issues associated with hydraulic fracturing, while also leading to improved production yields. Furthermore, it has been successfully applied to various unconventional gas reservoirs like coalbed methane, tight sandstone gas, and shale gas. Over the years, low-temperature nitrogen fracturing has emerged as a popular technique in hot and dry rock mining, overcoming restrictions imposed by water resources, avoiding reservoir pollution, preserving the reservoir, and effectively preventing dust. By utilizing low-temperature nitrogen, the free water in pores and fissures experiences frost swelling, creating significant rock cracks that result in the subsequent damage to the rock pore structure, thereby improving reservoir fracturing effects [6, 7]. Studying rock fracture behavior under the influence of liquid nitrogen damage is, therefore, of utmost importance. It offers a promising avenue for the efficient extraction of geothermal energy and presents a viable

alternative to hydraulic fracturing, especially in water-scarce areas rich in coal resources.

With the ongoing development of natural science and technology, many scholars have utilized various monitoring methods and instruments to conduct experiments and analyze the behavior of coal during different loading stages in the process of rock failure and instability. These studies have aimed to investigate various test parameters and have consistently resulted in comparable conclusions concerning both microscopic fracture characteristics and essential mechanics. As the rock undergoes stress and deformation, energy accumulates before microcracks and failures occur within the rock. The stored energy is then released in the form of acoustic emission (AE) waves as the load increases. AE monitoring has become a common nondestructive testing method that allows for accurate determination of the extent of damage sustained by rocks [8, 9]. The inception of modern AE technology is credited to Kaiser's research in Germany during the early 1950s. His observations led to the discovery of AE phenomena in the deformation process of metals and alloys and highlighted the "Kaiser effect" [10]. Later, American scholars, Gholizadeh et al. [11], studied AE phenomena during the plastic deformation and failure of metal materials and made a significant theoretical breakthrough by establishing that the volume effect is a crucial factor contributing to AE activity. Goodman further confirmed that rock materials experience a significant Kaiser effect during deformation and failure through indoor compression tests [12]. By employing AE monitoring techniques, it is possible to obtain valuable insights into the behavior of coal during different loading stages, providing critical information for improving our understanding of rock failure and instability. The advancement of AE technology has significantly contributed to nondestructive testing and has played an indispensable role in the field of geomechanical engineering.

Rong, a Chinese scholar, conducted various triaxial experiments using different loading methods and concluded that the acoustic emission behavior of rocks is not only related to their stress state but also to their stress pathway [13]. Furthermore, Zhao et al. [14] have systematically summarized the main research achievements both domestically and internationally on the generation mechanism of the Kaiser effect of AE on rock, the Kaiser effect point identification method, and the factors affecting the Kaiser effect. They have also proposed future research directions and content for the Kaiser effect on acoustic emission in rocks. Numerous scholars have extensively studied rock acoustic emission tests and strength fractal models that are widely used in significant rock engineering projects [15–20]. However, future research should focus on exploring the relationship between acoustic emission and rock deformation characteristics, surface features, and pore structure. To ensure accurate and reliable data collection, it is essential to develop suitable acoustic emission monitoring equipment and algorithms. In addition, developing new models for interpreting acoustic emission data would improve our understanding of the underlying mechanisms of acoustic emission in rocks. Future research should prioritize developing such models to obtain deeper insights into the behavior of rocks under different loading conditions. By doing so, scientific understanding can be advanced, and practical applications in geomechanical engineering can be improved.

Considerable research has been conducted on the effects of liquid nitrogen cycling on rock acoustic emission. For instance, Kumari et al. [21] examined the mechanical behavior of Strathbogie granite in Australia under uniaxial conditions using two cooling methods and analyzed the corresponding fracture propagation mode with an AE system. Similarly, Liu et al. [22] investigated two types of raw coal under different conditions, such as varying water content, temperatures, and freeze-thaw cycles. They employed multiple testing methods, including uniaxial compression tests, acoustic wave tests, and nuclear magnetic resonance imaging technology to investigate the variation characteristics of strength, elastic modulus, failure form, wave velocity, and internal crack propagation. By utilizing advanced technologies and methodologies, such as AE systems and nuclear magnetic resonance imaging, researchers have been able to gain deeper insights into the mechanical behavior of rocks under different loading conditions. The findings from these studies provide valuable information for geomechanical engineering and can aid in the development of effective strategies for rock failure prevention and control. Further research in this field should aim to explore new avenues for studying the effects of liquid nitrogen cycling on rock acoustic emission and developing new techniques for data analysis and interpretation.

Chu et al. [23] utilized infrared thermal imaging technology to examine the temperature distribution in coal samples following liquid nitrogen freezing. They subjected the samples to uniaxial compression and acoustic emission testing, both before and after undergoing the freeze-thaw cycle. The team then scrutinized the impact of velocity, porosity, acoustic emission, and energy evolution on the same samples. Furthermore, they endeavored to unveil the damage mechanism of coal samples that underwent liquid nitrogen freezing. Sun et al. [24] investigated the "fast-slow-fast-slow" decline pattern of central temperature in granite through theoretical analysis, physical experiments, and numerical simulation. Li et al. [25] developed a pore network model using 3D visualization software, demonstrating that the size of new pore cracks generated by liquid nitrogen freeze-thaw is smaller than those created by high-temperature heating. As a result, there is a gradual decrease in the proportion of large pores. Li et al. and Liu et al. conducted cold-loading experiments on coal samples with different joints, water saturation, initial temperature, confining pressure, and low temperature. He used laser confocal microscopy, ultrasonic detection analyzer, and CT scanning to investigate the changes in crack width, wave velocity attenuation, and porosity of coal samples. The structural damage evolution law of coal samples under cold loading was analyzed [26, 27]. Novikov et al. studied the acoustic emission response of fossil coal and revealed and analyzed the response characteristics of anthracite, bituminous coal, and lignite samples. He conducted research on fossil coals at different metamorphic stages to explore their response under effective thermal stress cycling [28]. Shkuratnik et al.'s experiments on

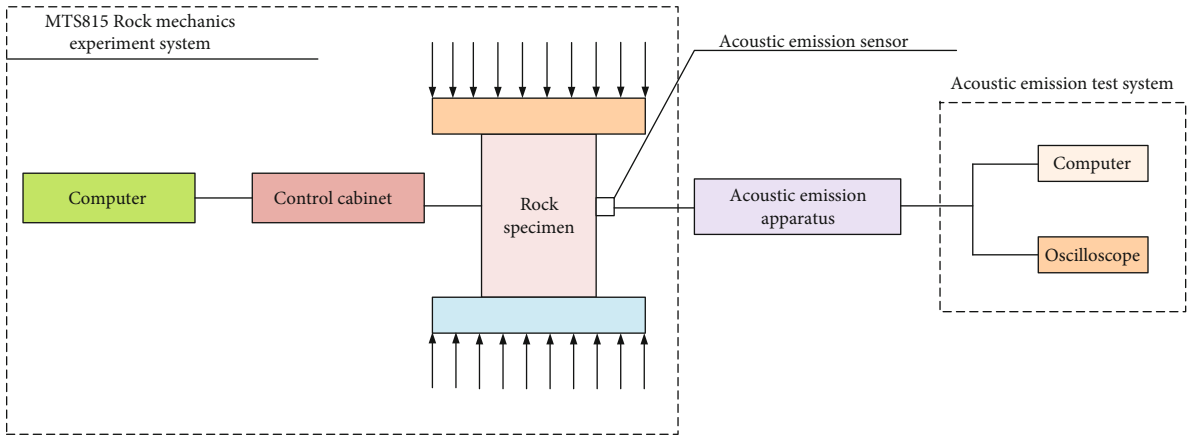

Figure 1: Acoustic emission monitoring system.

samples of different coal types exposed to various cyclic heating modes revealed the characteristics of the thermal emission memory effect that formed and manifested, depending on the magnitude and duration of the thermal field, through acoustic emission experiments [29]. In summary, many scholars have conducted extensive research on AE and the liquid nitrogen cycle, but relatively detailed studies on AE under the liquid nitrogen cycle are few.

This research focuses on coal as the central research object, and the rocks are tested using the Brazilian splitting test, followed by an AE analysis. The results indicate that liquid nitrogen has a significant impact on the generation and development of coal fractures under the conditions of the Brazilian splitting test. Additionally, we found that the combination of liquid nitrogen freezing and the Brazilian splitting test can further improve the accuracy of assessing the brittleness of coal. This technique can effectively evaluate the rock quality, providing guidance for the development and utilization of coal in the mining industry. Furthermore, using advanced imaging techniques and numerical modeling, we gained insights into the internal structural changes of coal after undergoing liquid nitrogen treatment. These findings are valuable in providing a comprehensive understanding of the fracture characteristics and damage mechanism of coal. Overall, the use of liquid nitrogen in coal testing has proven to be an effective and promising approach in the mining industry for improving the accuracy of assessing coal quality and enhancing safety. Future work should focus on exploring the potential and limitations of this technique and developing more practical applications in the field.

2. Experimental Procedures

2.1. Selection of Experimental Materials. After conducting thorough field investigations and comprehensive laboratory tests and reviewing the relevant findings from both domestic and foreign sources, this study investigated two types of coal mines. The MTS815 Flex Test GT rock mechanics loading system and the real-time three-dimensional positioning detection instrument PCI2 AE, developed by Acoustic Physics Company in the USA, were used in combination with an acoustic emission testing system. The study focused on investigating the fracture mechanism of coal under Brazilian splitting loading, while being subjected to the influence of liquid nitrogen, as illustrated in Figure 1. This approach allowed for a detailed and precise analysis of the impact of liquid nitrogen on the fracture behavior of coal, which is a significant challenge in rock mechanics research. By integrating advanced technologies and employing rigorous testing methods, this study provides valuable insights into the fundamental behavior of coal fractures and enhances our understanding of the effects of external factors on the stability of coal mines.

2.2. Cycle Cooling Treatment. In this study, XRD testing was utilized to analyze the mineral composition of coal samples. As coal is prone to oxidation at relatively high temperatures, its structure can become deteriorated. To investigate the behavior of two types of coal samples under freeze-thaw cycles of liquid nitrogen, the samples were subjected to heating at 80 degrees Celsius followed by cooling with liquid nitrogen in a cycle, repeated for 3, 5, 7, 9, and 15 cycles, respectively. Acoustic emission technology was employed to record and analyze the data during the tests.

The load-displacement image, load-ringing counting-cumulative-counting image, load-energy-cumulative-energy diagram, RA-AF scatter diagram, and RA-AF density diagram of the two coal samples were analyzed using the parameter analysis method. Additionally, a scatter diagram was produced for each loading stage, providing insights into the various characteristics and rules of tensile and shear cracks at each stage.

These analyses allowed for a comprehensive understanding of the mechanical properties of the coal samples under freeze-thaw cycles of liquid nitrogen treatment. This research provides a valuable contribution to the field of rock mechanics and enhances our understanding of the behavior of fractures in coal samples under different external conditions.

2.3. Experimental Process

2.3.1. Study the Technical Process. The research technical process of this paper is roughly shown in Figure 2.

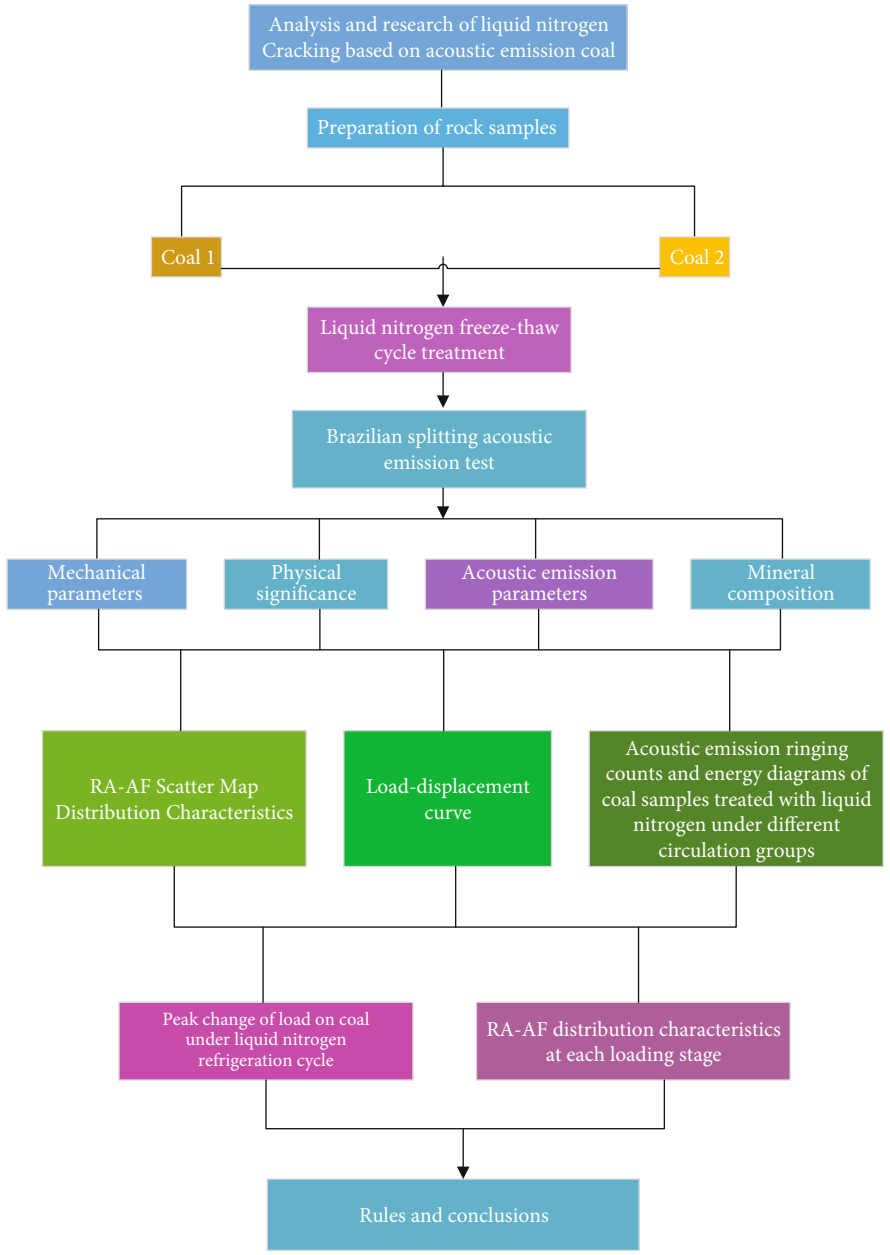

Figure 2: Research technical process.

2.3.2. Processing of Brazilian Split Sample and Its Principle. As the experimental method of Brazilian splitting is relatively simple, the tensile strength obtained by this method is often used to detect the tensile strength of coal both domestically and internationally, as it closely approximates the results obtained by direct tensile strength testing. The basic principle of the splitting method is derived from the elastic theoretical solution of coal-rock disks under diametral compression. During loading and failure of the coal sample, the maximum tensile stress occurs at the middle of the specimen and is given by

$$\sigma = \frac{2P}{\pi \mathrm{dt}}. \quad (1)$$

where σ is the maximum tensile stress in the middle of the coal sample, also known as tensile strength, and the symbol is MPa; P is the critical pressure when the coal sample is damaged, and the symbol is N. d and t are the diameter and thickness of the coal disk, respectively, and the symbol is mm.

In this study, the coal samples were pretreated in accordance with relevant regulations and standards before undergoing the Brazilian splitting test under liquid nitrogen freeze-thaw conditions. The samples were prepared as Brazilian disk samples with a thickness of 25 mm and a diameter of 50 mm. To reduce error, the maximum diameter error was kept within 0.1 mm across the entire thickness, while the nonparallelism of the two ends was kept within 0.1 mm. Additionally, the end face was required to be perpendicular to the axis of the specimen, with a maximum deviation of 0.25 degrees.

(a) Liquid nitrogen containers (b) Electronic universal testing machine

(c) Electric ovens (d) Acoustic emission equipment

Figure 3: Test equipment.

The equipment required for the test includes an electric oven and a liquid nitrogen container for the cooling process. A maximum sampling rate of 20000 pps was achieved using the CSS44100 electronic universal testing machine, PCI-2 automatic exposure monitoring system, and PCC 2.6 system. These instruments and equipment are shown in Figure 3.

Overall, these steps ensure the accuracy and reliability of the results obtained through the Brazilian splitting test under liquid nitrogen freeze-thaw conditions, contributing to a deeper understanding of the mechanical properties of coal samples.

2.3.3. Experimental Scheme. The Brazilian disk splitting test, commonly known as the Brazilian splitting test, is extensively used in the fields of applied mechanics and industrial engineering. In this study, coal samples were divided into two groups, namely, the temperature group and the cycle group, with the latter being the focus of research and analysis.

(1) *Sample Treatment.* The coal samples underwent two stages of treatment: liquid nitrogen freeze-thaw cycle treatment and the Brazilian splitting test. Firstly, the two types of coal samples were numbered, treated, and divided into "Untreated," 3, 5, 7, 9, and 15 cycles. The coal samples were then subjected to a cycle of cooling in liquid nitrogen (high-temperature heating refers to when the sample is heated to a predetermined temperature and then continuously heated for 3 hours, while liquid nitrogen cooling involves immersing the sample in liquid nitrogen for an hour each time), as illustrated in Figure 4. For the purpose of subsequent research and parameter analysis, the cycle groups were further divided into "untreated 1," "untreated 2," 3-1, 3-2, 5-1, 5-2, 7-1, 7-2, 9-1, 9-2, 15-1, and 15-2, and numbered in sequence

(2) *Experimental Loading Process.* After freezing and thawing the coal specimens in a liquid nitrogen cycle, the specimens were numbered and the color, grain, laminae, fractures, degree of weathering, and water content of the specimens were described and the dimensions measured with the Vernier calipers and recorded. The specimens are placed in the splitting jig after the freeze-thaw treatment with liquid nitrogen and secured with V-clamps and clamping screws on both sides. The splitting jig is placed in the upper and lower bearing plates of the electronic universal testing machine, keeping the center line of the coal specimen and the center line of the electronic universal testing machine in the same line, see Figure 5. Turn on the electronic universal testing machine, loosen the splitting clamps according to the double-side clamping screws, and then maintain a rate of about 0.4 MPa/s of applied load to apply the load evenly until the coal specimen is damaged. Then, record the splitting damage load for each group per cycle

After the experiment, the rock fracture can be observed as shown in Figure 6. The sample is coal that has undergone a Brazilian tensile strength test after five cycles of liquid nitrogen. It can be observed that obvious cracks have already appeared. These visible cracks suggest that the coal sample

Figure 4: Liquid nitrogen cycle operation process.

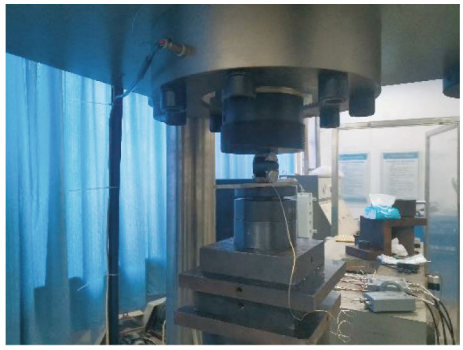

Figure 5: Operation diagram of the Brazilian splitting experiment.

may have reached its critical stress point and is prone to further fractures under mechanical or environmental pressure.

3. Mechanical Behavior of Coal

3.1. Study on Mechanical Behavior of Two Kinds of Coal. Through the experiment, a lot of information can be seen, and the law of destruction of coal is also revealed, reflecting the whole process of coal from the initial load to the final destruction. Originally, under the condition of Brazil splitting, the stress-strain graph should be drawn, but due to the time shortage and other reasons, the load-displacement graph is drawn to achieve the same effect. In addition, no matter the stress-strain graph or the load-displacement graph, the phenomenon and law of the mechanical effect of liquid nitrogen cycle freeze-thaw on coal samples under the condition of Brazil splitting can be obtained. Generally speaking, the load-displacement curve of coal will go through four different stages [30, 31].

(1) The first stage is the initial stage of crack generation, during which the stress is constantly loaded. In this stage, the stress is continuously loaded, with a certain nonlinear growth of downward sag, indicating that the stress increase is relatively slow

(2) The second stage is the stage of elastic deformation of the coal mass, and internal microcracks do not expand. At this time, the load-displacement curve presents a linear growth. It can be seen that some coal samples may reduce the load after experiencing the liquid nitrogen cycle, but it still presents a linear increase after the load increases

(3) The third stage is the crack propagation stage of coal. In this stage, inelastic deformation occurs in coal mass, microcracks are generated and gradually begin to expand, and new cracks are generated constantly. When the load gradually increases to the peak, microcracks in coal mass begin to integrate into macrocracks, and cracks increase constantly and, finally, lead to coal mass fracture

(4) The fourth stage is the stage of coal mass destruction, when the load reaches its peak, the coal mass begins to crumble, fail, and the stress begins to decrease

3.2. Summary of Mechanical Properties of Two Kinds of Coal. To better compare the changes in load-displacement in each group, we added a control group and remade the coal-rock control group to increase experimental randomness and accuracy of results. In subsequent acoustic emission experiments, we still focused on studying the two rock sample groups retrieved from Jiaozuo. The Brazilian splitting test was conducted on coal samples both before and after exposure to liquid nitrogen, and AE parameters with a time axis sequence were subsequently gathered. An error analysis was performed, and the maximum peak load in the three coal sample categories was obtained through careful evaluation and selection of the three critical parameters—load displacement. The results are presented in Table 1.

In order to facilitate data analysis and achieve better visual effect, the load-displacement diagram of the same coal sample is summarized, as shown in the following Figures 7–9.

Upon examination of each broken line independently and analyzing the chart generated by the first type of coal sample, it becomes evident that the highest and most significant load capacity of the coal samples, specifically the load at the time of failure, was achieved by the untreated samples. However, after three cycles of coal samples, the corresponding broken line's maximum peak value dropped significantly, indicating the impact of liquid nitrogen freeze-thaw on the Brazilian splitting test of coal. The examination of other loops showed that their maximum peaks decreased gradually, in contrast to the steep decrease observed from the untreated samples to those cycled three times.

To ensure the thoroughness and precision of the test, a second coal sample was utilized as a control, and AE parameters were acquired similarly. The resulting graph showed

Figure 6: Schematic diagram of coal failure state.

Table 1: Maximum peak load of the three samples without liquid nitrogen treatment and cyclic treatment.

Sample 1		Sample 2		Sample 3	
Number of cycles	Maximum peak load (N)	Number of cycles	Maximum peak load (N)	Number of cycles	Maximum peak load (N)
Untreated	1850	Untreated	1418.603	Untreated	1850.166
3	1200.164	3	1218.603	3	1208
5	1077.741	5	1145.873	5	820.34
7	828.778	7	773.951	7	768.418
9	820.34	9	623.669	9	670.673
15	678.909	15	504.592	15	500.64

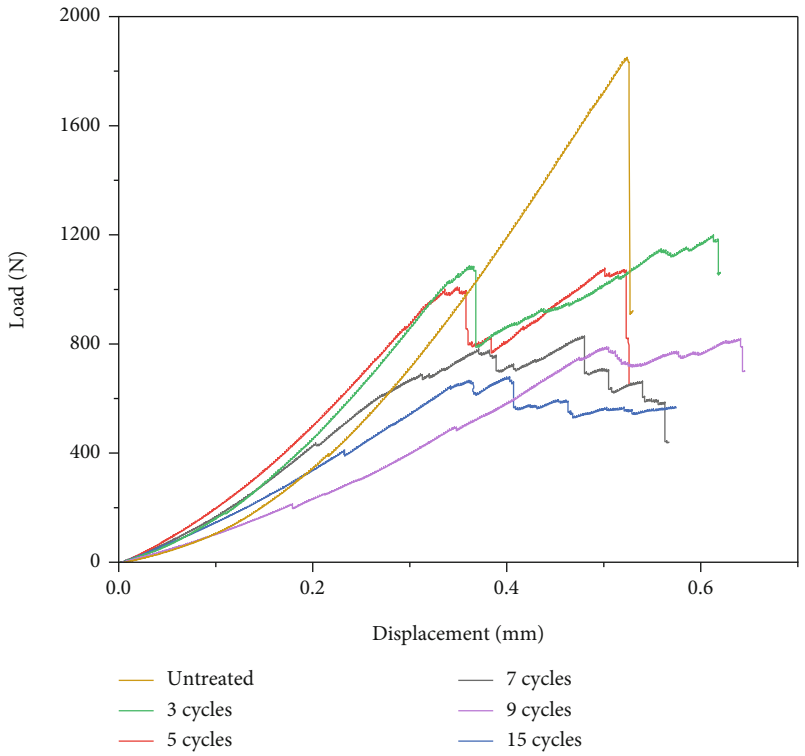

Figure 7: Load-displacement comparison between untreated and cyclic coal sample 1.

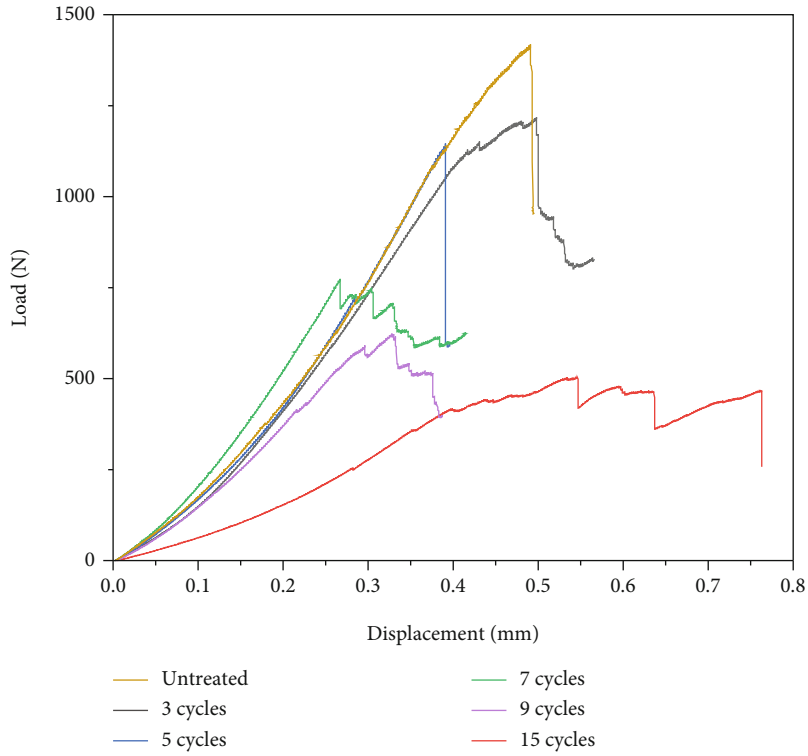

Figure 8: Load-displacement comparison between untreated and cyclic coal sample 2.

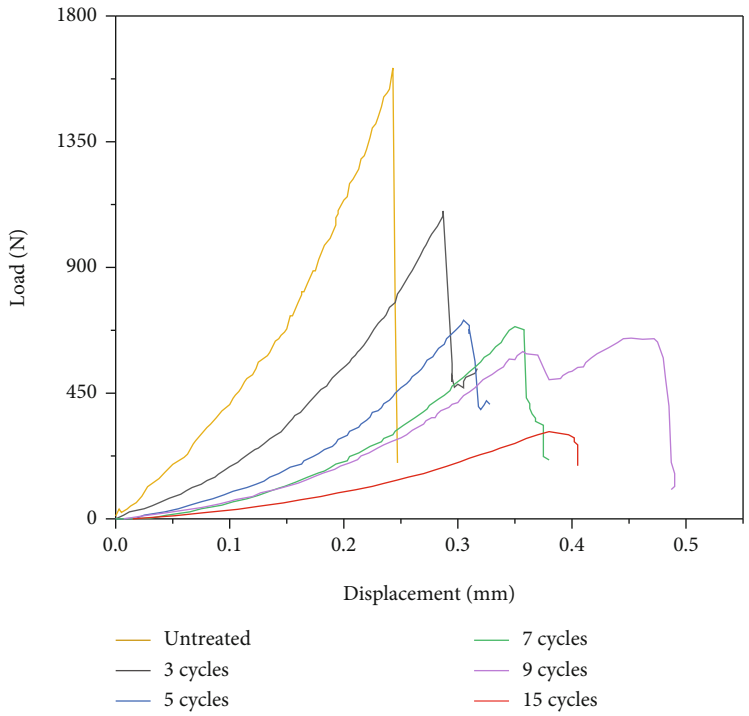

Figure 9: Load-displacement comparison between untreated and cyclic coal sample 3.

slight differences from the first type of coal, but the law obtained was essentially the same, validating the findings.

As for the overall graph, no matter the first sample or the second sample, after being treated with liquid nitrogen, with the increase of the number of freeze-thaw cycles of liquid nitrogen, the maximum load that the coal can bear gradually decreases, and the effective stress on the coal sample gradually decreases. In particular, the difference between

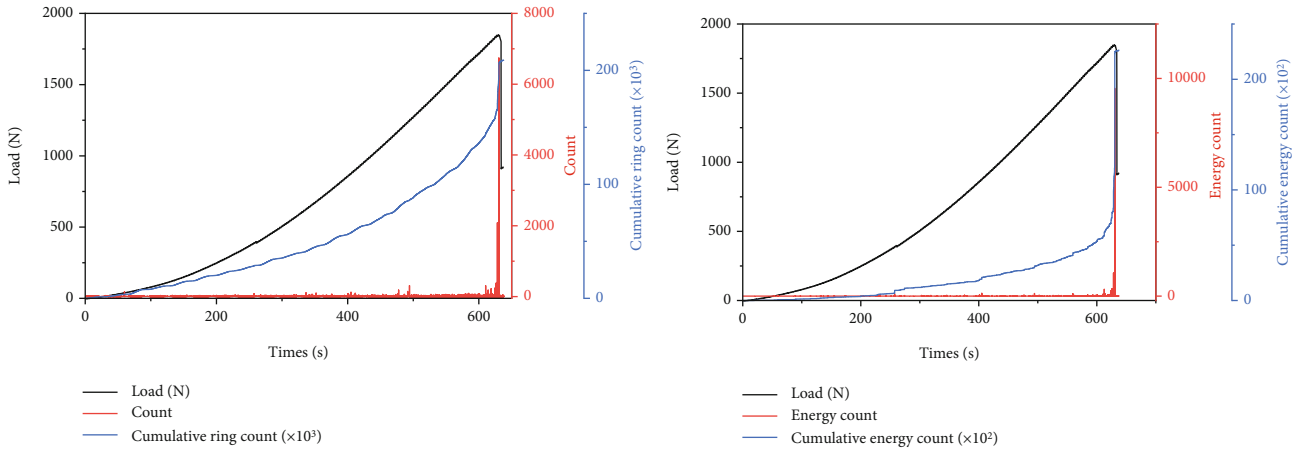

(a) Untreated

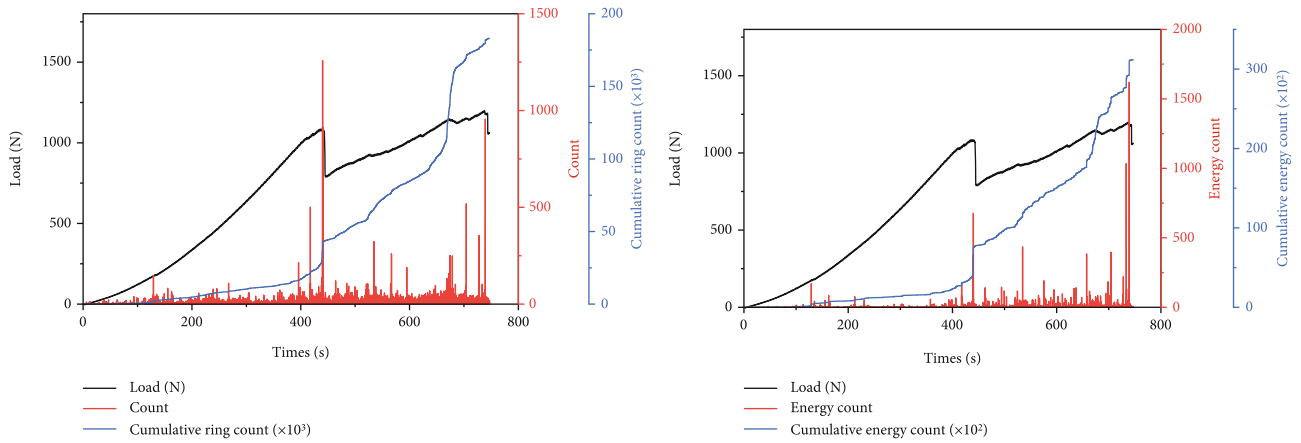

(b) 3 cycles

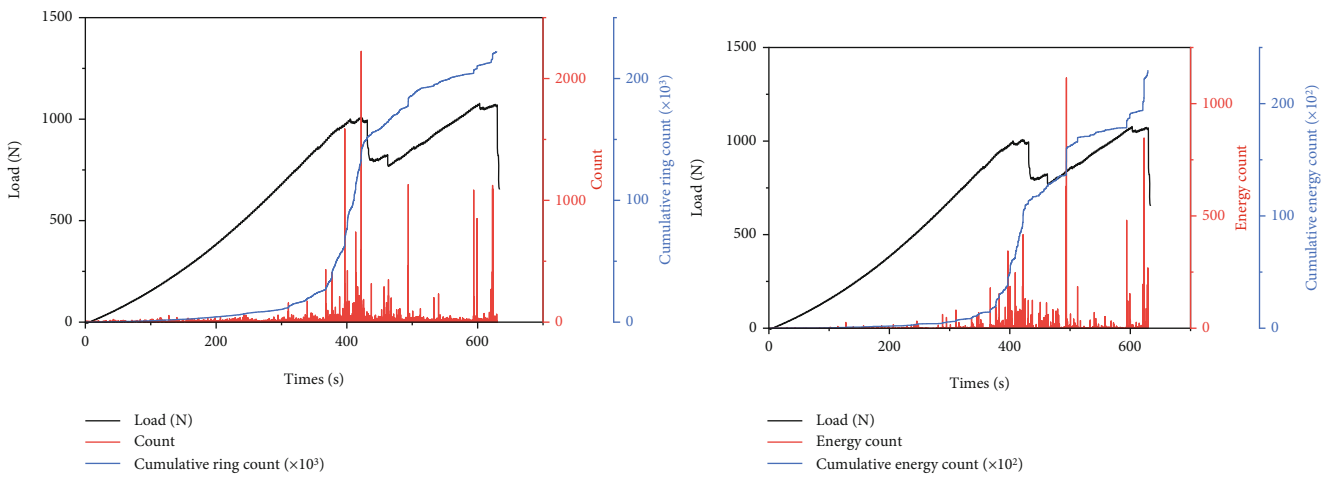

(c) 5 cycles

Figure 10: Continued.

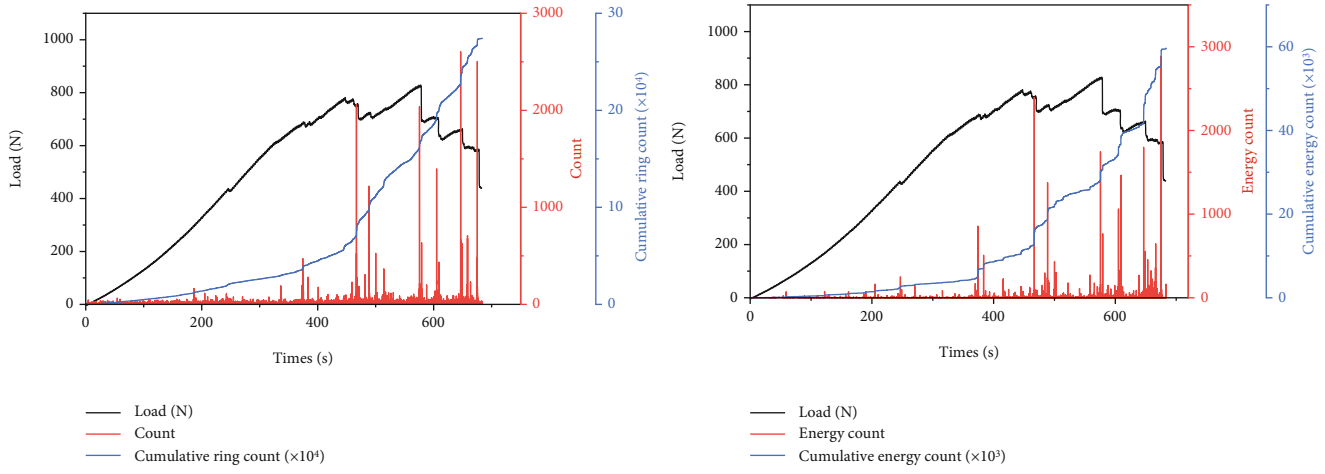

(d) 7 cycles

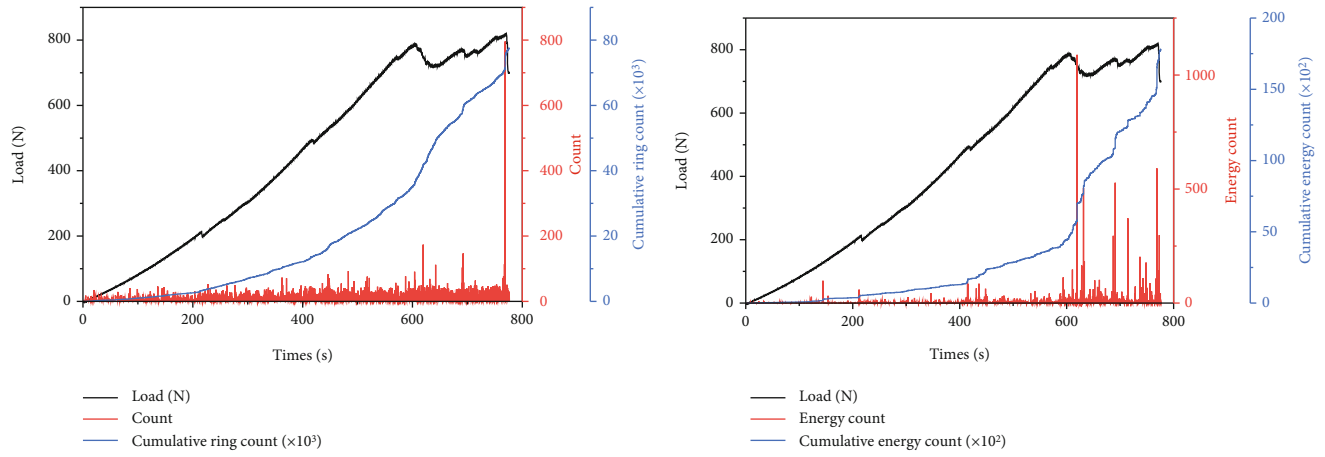

(e) 9 cycles

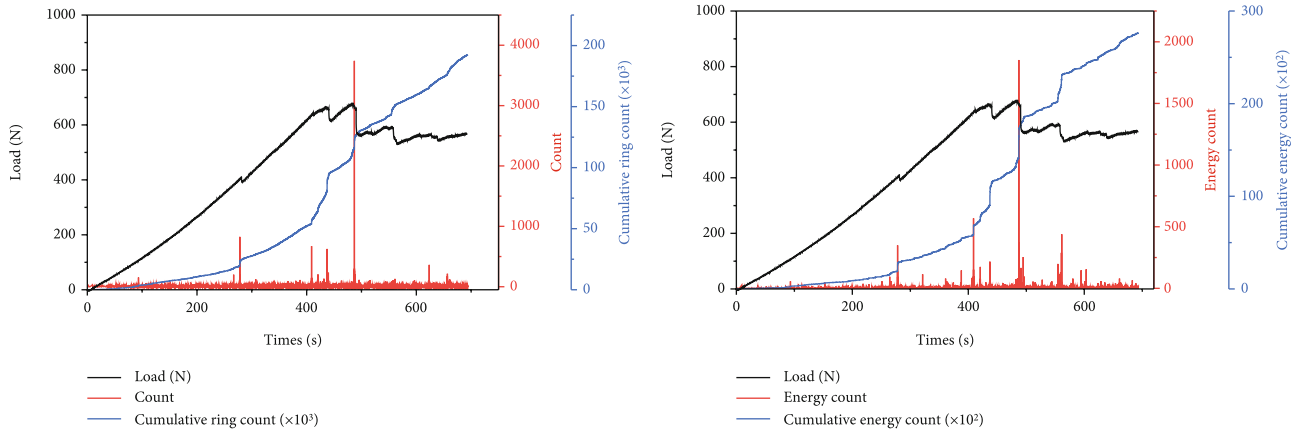

(f) 15 cycles

Figure 10: Loading-count-cumulative count and loading-energy-cumulative energy diagram of coal sample 1.

"untreated" and "treated with liquid nitrogen" is large. These experimental results demonstrate that the mechanical strength of coal samples continuously decreases after liquid nitrogen freeze-thaw cycle treatment. The reason for this phenomenon can be attributed to the microdamage and cracks caused by the internal structural changes of coal samples during the liquid nitrogen freeze-thaw process. These microdamages and cracks make the coal sample more susceptible to plastic deformation and failure, leading to a decline in the engineering performance of coal. Moreover, a prominent issue is that liquid nitrogen-treated coal samples are prone to higher strength impact.

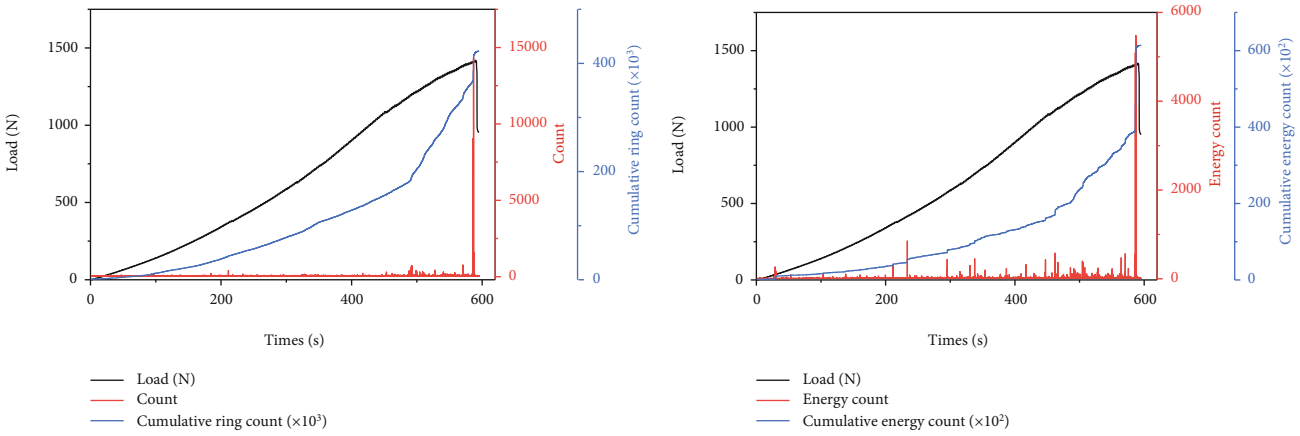

(a) Untreated

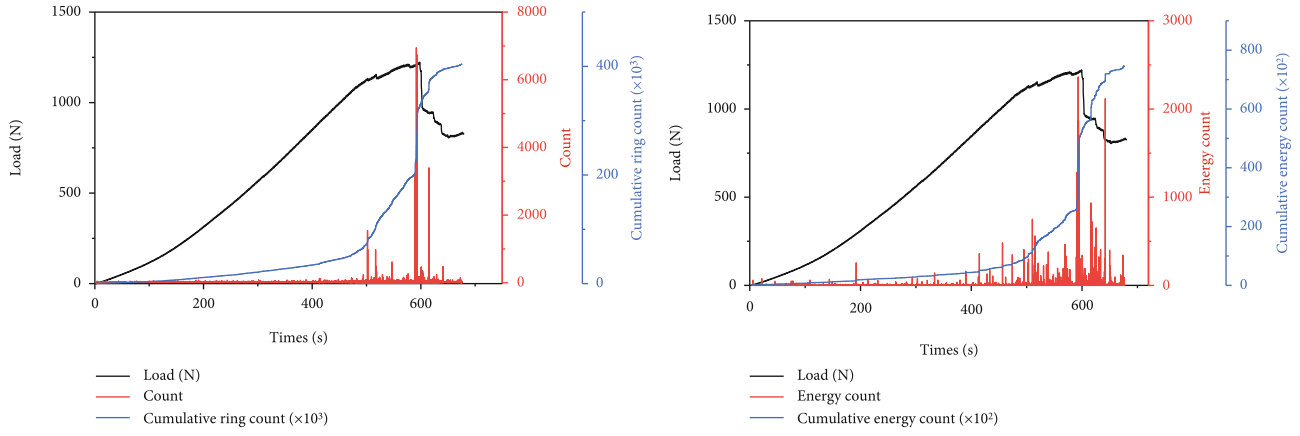

(b) 3 cycles

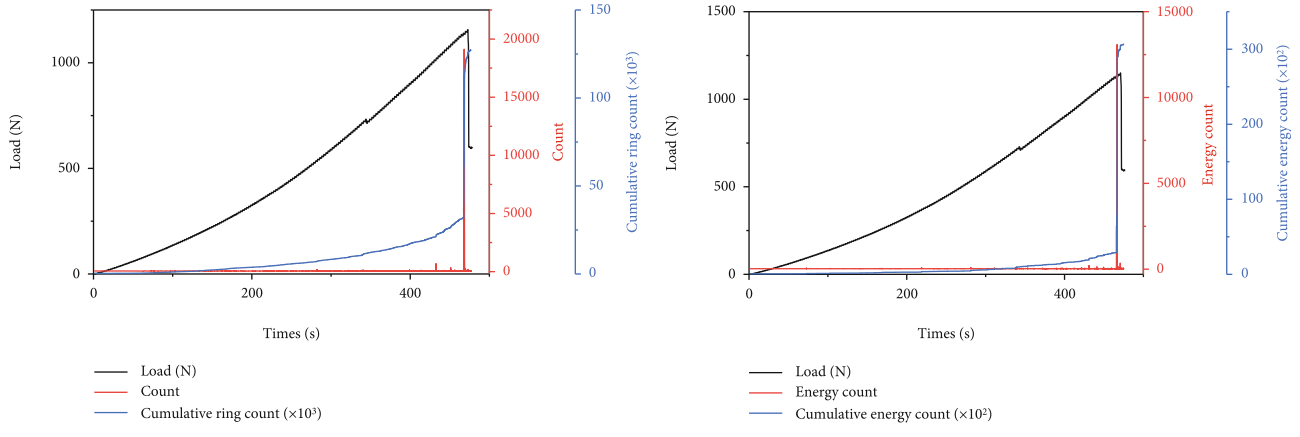

(c) 5 cycles

Figure 11: Continued.

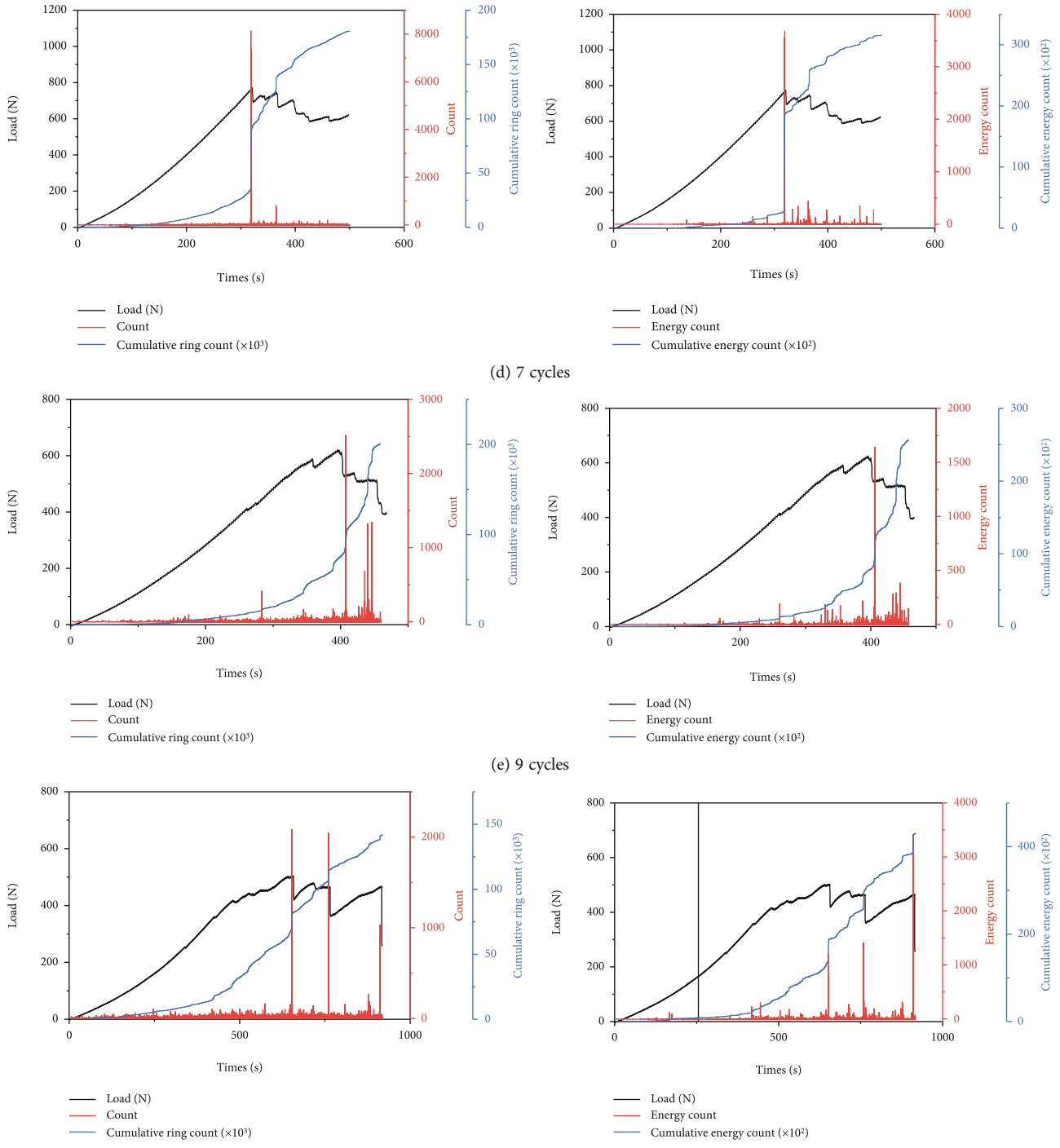

Figure 11: Loading-count-cumulative count and loading-energy-cumulative energy diagram of coal sample 2.

Therefore, in practical engineering applications, attention should be paid to the strength changes that may occur in coal samples after undergoing liquid nitrogen freeze-thaw cycle treatment.

4. Analysis of AE Characteristics of Coal

4.1. Experimental Results of Acoustic Emission Characteristics. The load-displacement acoustic emission curves obtained from the Brazilian splitting test reveal that coal exhibits significant acoustic emission activities during various stages of fracture. Throughout the load application process, coal demonstrates a consistently high level of AE activity. The AE parameters of two coal samples were analyzed by utilizing parameter analysis methodology, and the results were plotted in Origin drawing software. Figure 10(a) represents the loading-count-cum-count graph for sample 1, which did not undergo cyclic treatment. Figures 10(b)–10(f) demonstrate

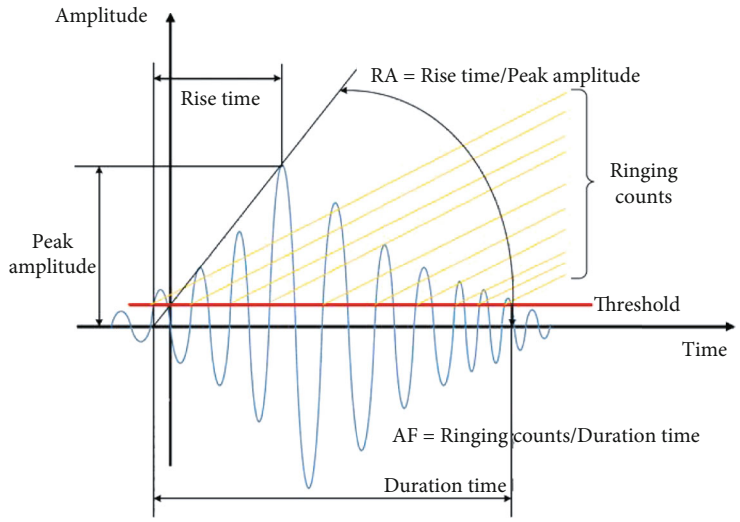

Figure 12: Typical waveforms and calculation of acoustic emission parameters.

the liquid nitrogen cycle freeze-thaw diagrams of sample 1. In order to validate and ensure the reliability of the testing, the second coal sample was also subjected to identical treatment and compared against sample 1. Figure 11 displays the processed images of the second coal sample. Figure 11(a) represents the untreated image, while Figures 11(b)–11(f) represent the liquid nitrogen cycle freeze-thaw diagram of the second sample.

Moreover, it is essential to note that the results showed a significant variation in the AE activity between the two coal samples, where the cumulative counts and energy of the treated sample were substantially higher, signifying a decrease in the coal's mechanical strength. Based on these outcomes, it is suggested that coal's exposure to liquid nitrogen cycles leads to its deterioration and reduces its structural properties. Therefore, it is necessary to adopt alternative measures to minimize the detrimental impact of the freezing and thawing process on coal.

At the first stage, that is, in the early stages of the development of fractures, it can be noted that there is little acoustic emission activity. In the second stage, elastic deformation occurs in coal mass, and a small amount of AE signal is generated in this stage, which has a low energy and a long duration. In the third stage, that is, the period of inelastic deformation of coal mass, AE signals are generated in large quantities at this stage. AE signals are very dense and their energy increases gradually. When the load reaches its peak, the AE signal energy also reaches its peak. In the fourth stage, after the stress reaches its peak, in the breakdown phase, acoustic emission activity remains active, but energy begins to decrease.

Regarding ringing count, it is evident that as the number of liquid nitrogen freeze-thaw cycles increases, the ringing count of circulating coal samples increases significantly. Moreover, with an increasing number of cycles, the AE activity intensity of coal samples also increases throughout each stage of fracture, plasticity, compaction, and elasticity. For instance, in Figure 10, the AE intensity gradually

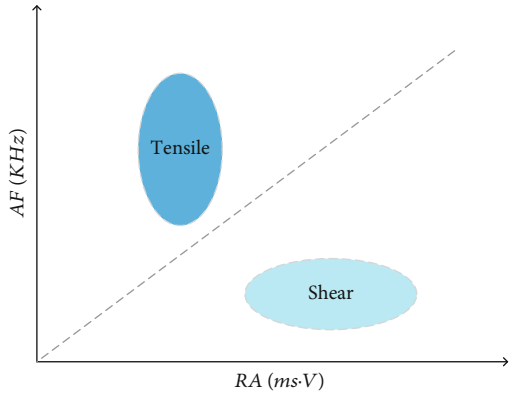

Figure 13: JCMS-IIIB5706 classification.

increases from Figures 10(a)–10(c), 10(e), and 10(f). The AE signal during coal fracture reflects the degree of activity within the coal, and as the number of cycles increases gradually, some areas will experience damage.

When a load is applied, the AE ringing count will sharply increase, resulting in a surge in the cumulative ringing count curve. In summary, liquid nitrogen freeze-thaw cycle treatment can fully leverage the cracking effect of liquid nitrogen, activate the original damage potential of coal, and improve damage distribution thus affecting the characteristics of coal.

In terms of energy, four overlifts corresponding to 20%, 50%, 60%, and 80% of peak load were observed. Acoustic emissions (AE) ringing count and energy of coal samples before and after liquid nitrogen treatment were analyzed. The results indicate that coal samples treated with liquid nitrogen show increased AE ringing count and energy values compared to untreated coal samples during the compaction stage. However, the probability of this situation gradually decreases with time. Initially, AE events occur between the coal mass and loading plate followed by internal crack closure resulting in AE activity during the elastic phase. During the fracture

Table 2: Maximum peak load and load ratio data of untreated and liquid nitrogen cycles in coal 1.

Number of cycles	0.2 F	0.4 F	0.6 F	0.8 F	Maximum peak load (N)
Untreated	370.1332	740.2664	1110.3996	1480.5328	1850.666
3	240.0328	480.0656	720.0984	960.1312	1200.164
5	215.5482	431.0964	646.6446	862.1928	1077.741
7	165.7556	331.5112	497.2668	663.0224	828.778
9	164.068	328.136	492.204	656.272	820.34
15	135.7818	271.5636	407.3454	543.1272	678.909

Table 3: Maximum peak load and load ratio data of untreated and liquid nitrogen cycles in coal 2.

Number of cycles	0.2 F	0.4 F	0.6 F	0.8 F	Maximum peak load (N)
Untreated	283.729	567.458	851.187	1134.916	1418.645
3	243.7206	487.4412	731.1618	974.8824	1218.603
5	229.1746	458.3492	687.5238	916.6984	1145.873
7	154.7902	309.5804	464.3706	619.1608	773.951
9	124.7338	249.4676	374.2014	498.9352	623.669
15	100.9184	201.8368	302.7552	403.6736	504.592

stage, there is a continued increase in applied pressure leading to more active AE activity until the coal sample is destroyed. After the peak stage, the coal samples enter the failure stage, the load drops abruptly, and the AE activity also decreases. The AE accumulated energy and load curves show a parallel upward state, with a jump phenomenon occurring during each stage of the peak load and after the peak. However, the jump phenomenon suggests that the stress state inside the coal did not reach a balance after coal sample cracks formed until it was destroyed, leading to AE generation. Once the stress state reached a balance, AE events reduced to zero.

Regarding continuing this article, further research can be conducted to study the effects of different liquid nitrogen temperatures on the acoustic emissions of coal samples. This can be done by conducting experiments with different temperature treatment groups and measuring the AE ringing count and energy values of coal samples during the compaction, elastic, and fracture stages. Additionally, the research can be extended to investigate how acoustic emission monitoring can be used to detect and predict coal sample failure. This can help in developing better methods for predicting coal sample failure, which would be useful in the coal mining industry, where safety and risk management are of utmost importance.

4.2. Crack Classification Study

4.2.1. Crack Classification Method. Figure 12 displays the waveform diagram of the general acoustic emission signal, while Equations (2) and (3) outline the calculation of AE parameters. These AE characteristic parameters comprise time, ringing count, duration, amplitude, and energy. Previous research has established that RA and AF are two crucial AE parameters. It is important to note that during the processing of AE parameters, the unity of the resultant parameter units should be ensured. In case the units differ, conversion of values is necessary to ensure the accuracy of the data. Without proper conversion, the utilization of data with variant units may lead to erroneous conclusions.

In the above waveform, AE parameter RA refers to the ratio of rise time to amplitude, expressed in ms/v.

$$\mathrm{RA} = \frac{\text{Rise time}}{\text{Amplitude}}. \tag{2}$$

The AE parameter AF value is the ratio of ringing count and duration, expressed in KHz.

$$\mathrm{AF} = \frac{\text{Counts}}{\text{Ring time}}. \tag{3}$$

Up to now, numerous scholars have utilized JCMS-IIIB5706 to categorize rock cracks. This technique employs AE parameters, RA and AF, for classification by computing the ratio of ring count to duration and the ratio of rise time and amplitude. The generated cracks in coal are then sorted into tensile and shear cracks based on the correlation between RA and AF, as illustrated in Figure 13. Nonetheless, the specific ratio between the standard and RA and AF remains unclear.

RA value and AF value can map the crack types in coal structure. Generally, low RA value and high AF value indicate that the crack is mainly affected by tensile action. Similarly, when RA value is high and AF value is low, it indicates that the crack is mainly affected by shear action. Therefore, on the basis of combining the failure characteristics, this method can analyze the occurrence and expansion of coal specimen cracks under different load conditions.

4.2.2. Crack Analysis Based on AE Parameters in Brazil Test. According to the crack classification method in 4.2.1, cracks

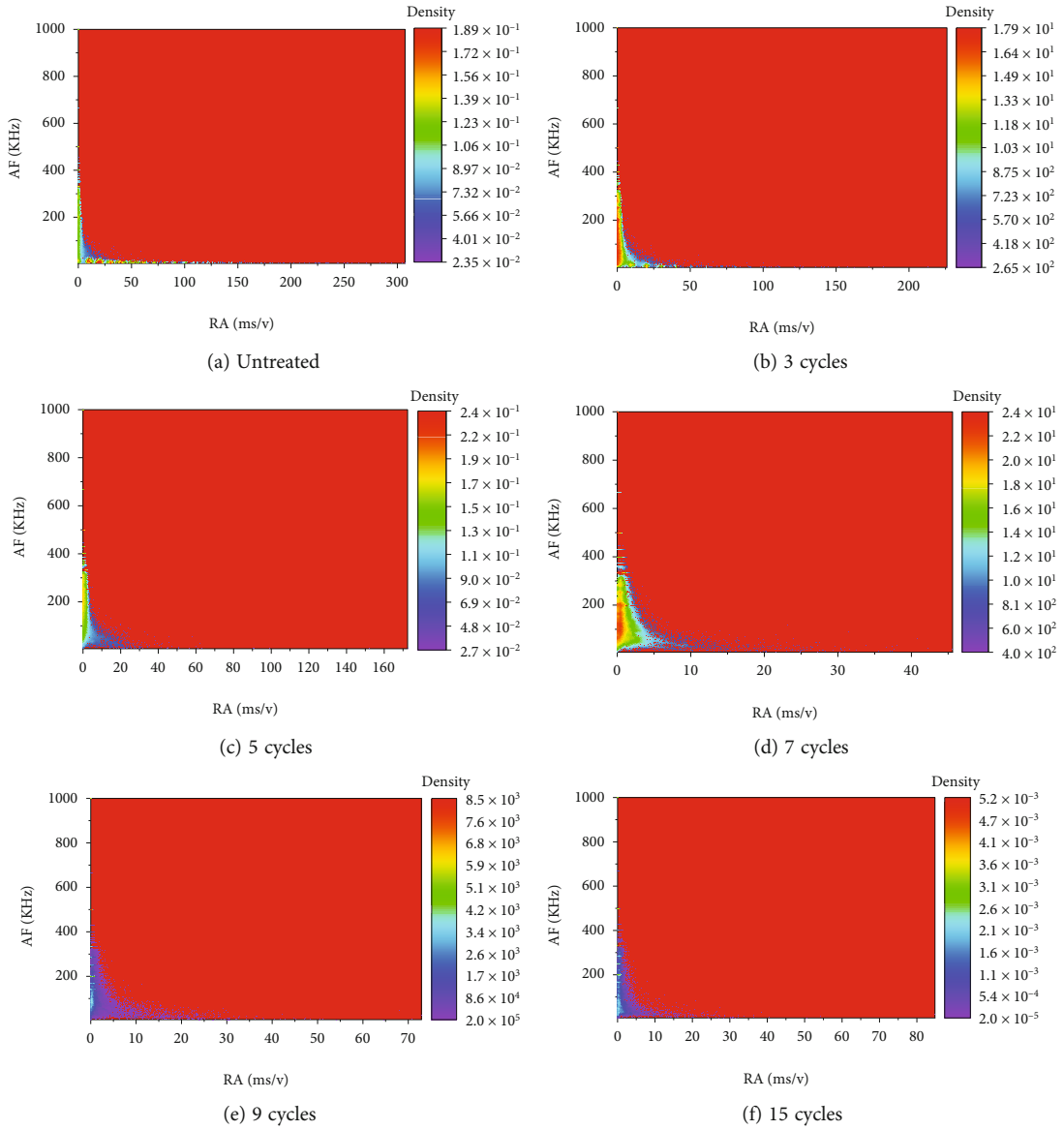

Figure 14: Distribution density of coal 1 after different cycle treatments.

generated in the Brazilian splitting process of coal samples are classified. Meanwhile, drawing software is used to make the distribution diagram of data coordinate points of RA-AF, and the scattered image corresponding to each peak load proportion is drawn.

According to the parameter analysis method, the ringing count, amplitude, rise time, and duration in the AE parameters of the coal sample were analyzed, and the RA value and AF value of the new AE parameter were obtained. The new AE parameters, RA and AF values, were obtained. Plot a plane with RA as the horizontal axis and AF as the vertical axis. The maximum load peak of AE parameters obtained without liquid nitrogen treatment and cyclic treatment was recorded, and 0.2, 0.4, 0.6, and 0.8 of the maximum load and the maximum peak load were taken. These are shown in Tables 2 and 3.

In order to analyze the distribution difference of RA-AF with different cycles of coal samples under the condition of Brazilian splitting, two RA-AF graphs without liquid nitrogen treatment and different cycles of liquid nitrogen were plotted, as shown in Figures 14 and 15:

It can be seen from the RA-AF distribution density diagram of the first type of coal samples without liquid nitrogen treatment that the distribution density is concentrated near the Y axis, where the distribution density of 0 to 400 KHz in the AF axis is larger, and the farther away from the Y axis the scatter density is, the lower it is. In conclusion, the distribution density is the radiation center from 0 to 400 KHz along the Y-axis, with high distribution density in the center and low distribution density around it. In order to ensure the rigor and universality of the liquid nitrogen cycle treatment test of coal, a second sample of coal was set up for comparison, and similar crack characteristics were obtained.

Next, the scatter distribution diagram of each loading stage of the same group is analyzed, and the coal 1 untreated,

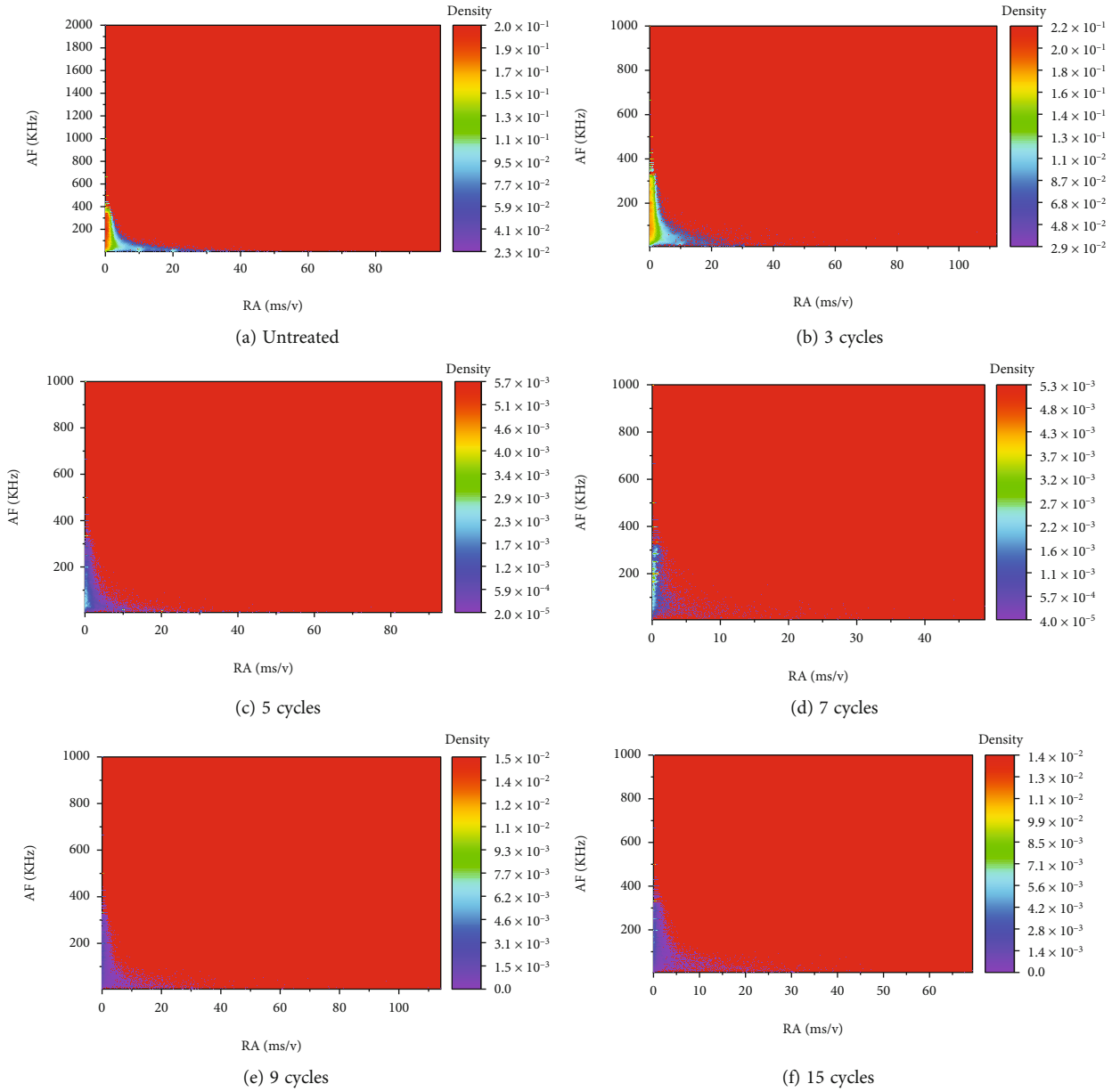

Figure 15: Distribution density of coal 2 after different cycle treatments.

3 cycles, and 9 cycles are taken as control analysis, as shown in Figure 16.

Observing the scatter distribution diagram of each loading stage in the same group, we found that the scatter is primarily located above the slash near the AF axis. As the applied load increased, the proportion of scatter points below the slash line gradually increased, as demonstrated in Figure 16; three types of cycles (a), (b), and (c) are presented, where the proportion of scatter points increases from (1) to (5). The distribution pattern of the scatter remained consistent, predominantly above the slash line and progressively denser.

Based on the classification of cracks in coal showcased in Figure 14, the gradual loading of coal samples mainly led to the germination, extension, and failure of tensile cracks. The development, extension, and failure of shear cracks are secondary. Nevertheless, with an increase in applied load, shear cracks became more prevalent, increasing the proportion of secondary effects.

Looking at other liquid nitrogen cycling treatment groups of the same coal-rock sample, it is observed from the scatter distribution diagram at each loading stage that with the increase of liquid nitrogen freeze-thaw cycles, the influence laws of tensile cracks and shear cracks are roughly consistent, with more scatter points of high RA and low AF, and fewer scatter points of low RA and high AF. The results reveal that the liquid nitrogen treatment significantly alters the distribution of cracks in coal samples, thereby impacting their behavior under loading conditions.

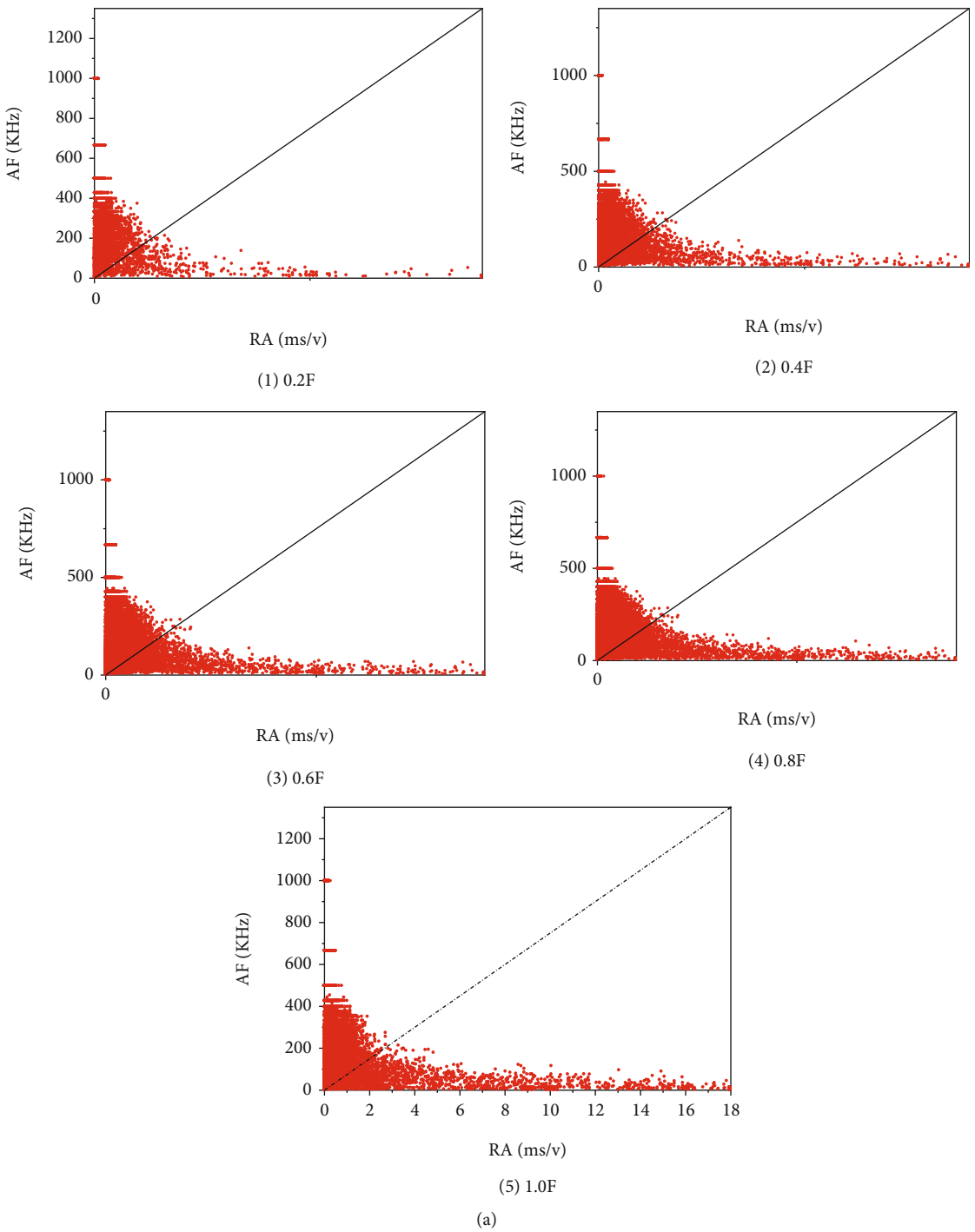

Figure 16: Continued.

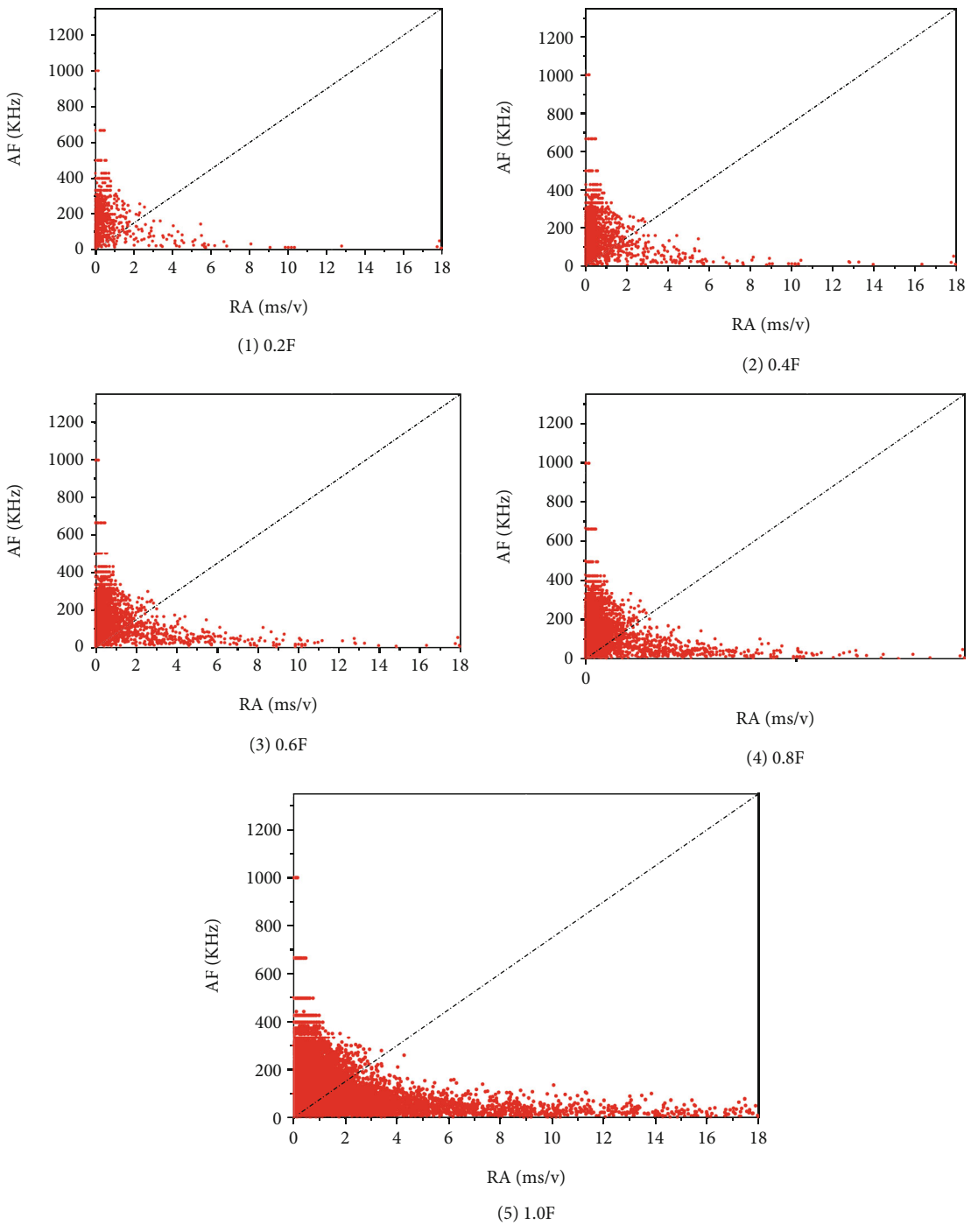

Figure 16: Continued.

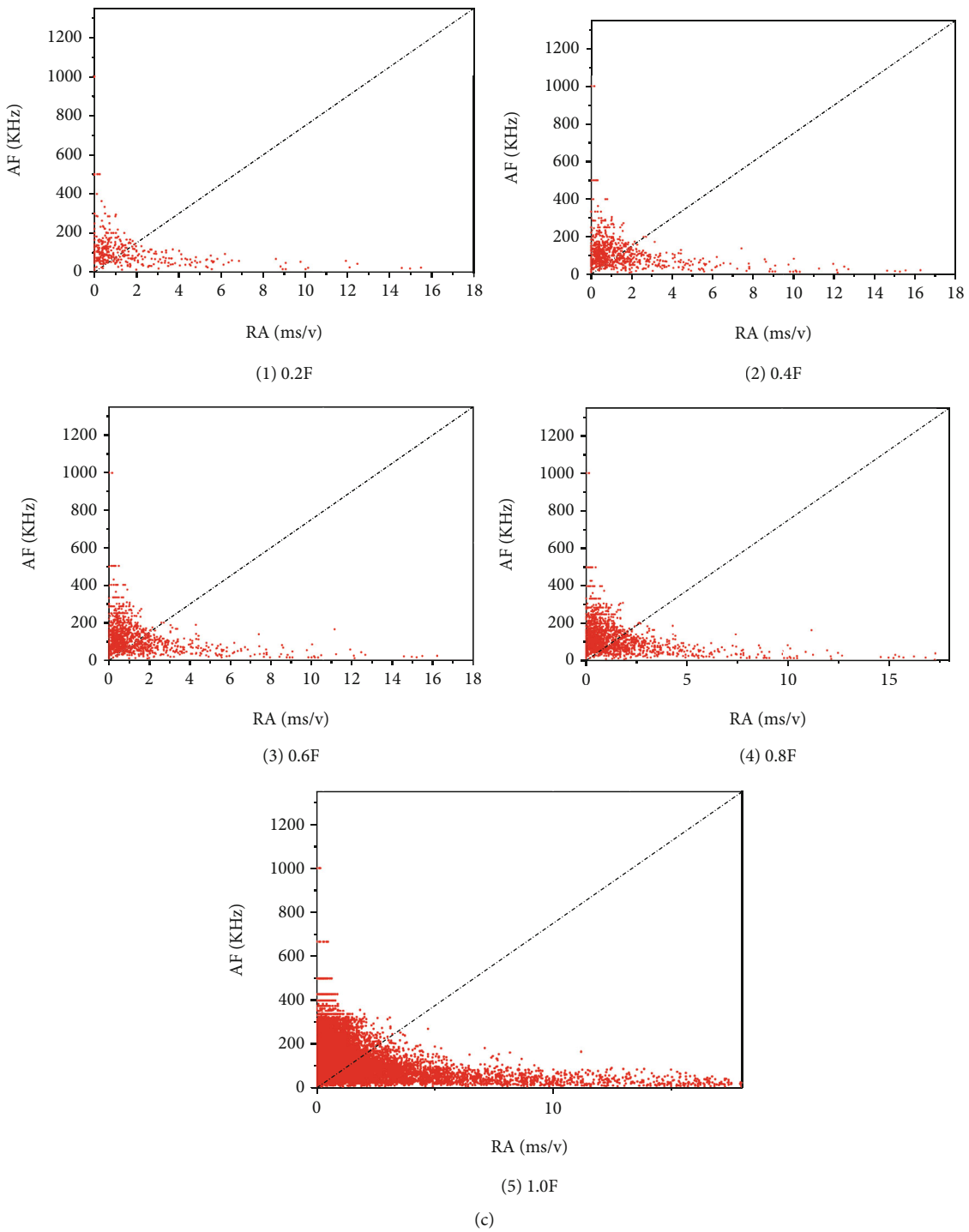

Figure 16: Scattered distribution diagram of coal 1 at different stages under different cycles. (a) untreated; (b) 3 cycles; (c) 9 cycles.

5. Conclusion

After the preparation of coal samples and the freeze-thaw cycle processing of liquid rock, various AE parameters were obtained, and the drawing software Origin was used to draw and the feature law of the images was analyzed. The following conclusions could be drawn:

(1) From the relation of load displacement, after the liquid nitrogen freeze-thaw treatment, as the number of liquid nitrogen freeze-thaw cycles increases, the maximum load value that the coal can bear gradually decreases, that is, the effective stress on the coal sample gradually decreases, especially the difference between the maximum load peak value

of the "untreated" and "treated with liquid nitrogen" is large

(2) From the parameter graph analysis of ringing count and energy, it can be seen that as the number of liquid nitrogen freeze-thaw cycles increases, the AE activity intensity of coal mass increases in the four loading stages: compaction stage, elastic stage, plastic stage, and fracture stage. After the application of load, the AE ringing count will increase sharply, resulting in a surge in the cumulative ringing count curve. Liquid nitrogen freeze-thaw cycle treatment can give full play to the cracking effect of liquid nitrogen, stimulate the original damage potential of coal, and improve the damage distribution will influence the mechanical properties of coal

(3) In the process of gradual loading of coal samples, the main factor is the germination, extension, and failure of tensile crack, and the secondary factor is the development, extension, and failure of shear crack. However, with the increase of applied load, the proportion of secondary effect, namely, shear effect, increases gradually. High RA and low AF have more scattered points, while low RA and high AF have fewer scattered points

Data Availability

The data used to support the findings of this study are included within the article.

Conflicts of Interest

The authors declare that they have no conflicts of interest.

Acknowledgments

The authors are grateful to the financial support from the National Natural Science Foundation of China (52274096, 51679199, 51979225, 51909204, 42007264, and 12002270), the Special Funds for Public Industry Research Projects of the Ministry of Water Resources (201501034-04), the Key Laboratory for Science and Technology Coordination and the Innovation Projects of Shaanxi Province (2014SZS15-Z01), the Key Research and Development Program of Shaanxi Province, China (2022ZDLSF07-02, 2022ZDLSF07-06, and 2023-YBSF-369), the Natural Science Basic Research Program of Shaanxi (2022JC-LHJJ-08), the China Postdoctoral Science Foundation (2020M683686XB, 2020M673451, 2021T140553, and 2021M692600), and the Youth Talent Promotion Project of the Xi'an Association for Science and Technology (095920211334).

References

[1] Z. Z. Wang, C. H. Ou, and H. Y. Wang, "The characteristics and development of geothermal resources in China," *Water Resources and Hydropower Engineering*, vol. 50, no. 6, p. 187, 2019.

[2] K. F. Evans, F. H. Cornet, T. Hashida et al., "Stress and rock mechanics issues of relevance to HDR/HWR engineered geothermal systems: review of developments during the past 15 years," *Geothermics*, vol. 28, no. 4-5, pp. 455–474, 1999.

[3] Y. Xue, S. Liu, J. Chai et al., "Effect of water-cooling shock on fracture initiation and morphology of high- temperature granite: application of hydraulic fracturing to enhanced geothermal systems," *Applied Energy*, vol. 337, article 120858, 2023.

[4] L. Gandossi and U. Von Estorff, *An Overview of Hydraulic Fracturing and Other Formation Stimulation Technologies for Shale Gas Production*, Eur. Commisison Jt. Res. Cent. Tech. Reports, 2013.

[5] D. Zhang and Y. Tingyun, "Environmental impacts of hydraulic fracturing in shale gas development in the United States," *Petroleum Exploration and Development*, vol. 42, no. 6, pp. 876–883, 2015.

[6] H. Akhondzadeh, A. Keshavarz, F. U. R. Awan, A. Z. Al-Yaseri, S. Iglauer, and M. Lebedev, "Coal fracturing through liquid nitrogen treatment: a micro-computed tomography study," *The APPEA Journal*, vol. 60, no. 1, pp. 67–76, 2020.

[7] Y. Xue, P. G. Ranjith, F. Gao, Z. Zhang, and S. Wang, "Experimental investigations on effects of gas pressure on mechanical behaviors and failure characteristic of coals," *Journal of Rock Mechanics and Geotechnical Engineering*, vol. 15, no. 2, pp. 412–428, 2023.

[8] V. A. Mansurov, "Acoustic emission from failing rock behaviour," *Rock Mechanics and Rock Engineering*, vol. 27, no. 3, pp. 173–182, 1994.

[9] D. A. Filipussi, C. A. Guzmán, H. D. Xargay, C. Hucailuk, and D. N. Torres, "Study of acoustic emission in a compression test of andesite rock," *Procedia Materials Science*, vol. 9, pp. 292–297, 2015.

[10] E. J. Kaiser, *A Study of Acoustic Phenomena in Tensile Test*, Dr.-Ing. Dissertation. Technical University of Munich, 1950.

[11] S. Gholizadeh, Z. Leman, and B. T. H. T. Baharudin, "A review of the application of acoustic emission technique in engineering," *Structural Engineering and Mechanics*, vol. 54, no. 6, pp. 1075–1095, 2015.

[12] R. E. Goodman, "Subaudible noise during compression of rocks," *Geological Society of America Bulletin*, vol. 74, no. 4, pp. 487–490, 1963.

[13] C. Rong, "Acoustic emission of rocks under triaxial compression with various stress paths," *International Journal of Rock Mechanics and Mining Sciences & Geomechanics Abstracts*, vol. 16, no. 6, pp. 401–405, 1979.

[14] Z. Kui, X. Weibin, Z. Peng et al., "Research status and prospect of Kaiser effect in rock acoustic emission," *Metal Mine*, vol. 50, no. 1, p. 94, 2021.

[15] A. Carpinteri, G. Lacidogna, F. Accornero, A. C. Mpalaskas, T. E. Matikas, and D. G. Aggelis, "Influence of damage in the acoustic emission parameters," *Cement and Concrete Composites*, vol. 44, pp. 9–16, 2013.

[16] A. Carpinteri, G. Lacidogna, and S. Puzzi, "From criticality to final collapse: evolution of the " _b_ -value" from 1.5 to 1.0," *Chaos, Solitons & Fractals*, vol. 41, no. 2, pp. 843–853, 2009.

[17] K. Du, X. Li, M. Tao, and S. Wang, "Experimental study on acoustic emission (AE) characteristics and crack classification during rock fracture in several basic lab tests," *International Journal of Rock Mechanics and Mining Sciences*, vol. 133, article 104411, 2020.

[18] S. Q. Yang, H. W. Jing, and S. Y. Wang, "Experimental investigation on the strength, deformability, failure behavior and acoustic emission locations of red sandstone under triaxial compression," *Rock Mechanics and Rock Engineering*, vol. 45, no. 4, pp. 583–606, 2012.

[19] H. R. Hardy, "Application of acoustic emission techniques to rock mechanics research," *Acoustic Emission, ASTM STP*, vol. 505, pp. 41–83, 1972.

[20] Y. Xue, J. Liu, X. Liang et al., "Influence mechanism of brine-gas two-phase flow on sealing property of anisotropic caprock for hydrogen and carbon energy underground storage," *International Journal of Hydrogen Energy*, vol. 48, no. 30, pp. 11287–11302, 2023.

[21] W. G. P. Kumari, P. G. Ranjith, M. S. A. Perera, B. K. Chen, and I. M. Abdulagatov, "Temperature-dependent mechanical behaviour of Australian Strathbogie granite with different cooling treatments," *Engineering Geology*, vol. 229, pp. 31–44, 2017.

[22] N. Liu, L. Sun, B. Qin, S. Zhang, and W. Du, "Evolution of pore and fracture of coal under heating-freezing effects: an experimental study," *Fuel*, vol. 306, article 121618, 2021.

[23] Y. Chu, J. Zhang, D. Zhang, M. Wang, Y. Wang, and Z. Niu, "Experimental study on the fissure structure and permeability evolution characteristics of coal under liquid nitrogen freezing and freeze–thaw," *Physics of Fluids*, vol. 34, no. 12, article 126601, 2022.

[24] Y. Sun, C. Zhai, J. Xu et al., "Damage and failure of hot dry rock under cyclic liquid nitrogen cold shock treatment: a non-destructive ultrasonic test method," *Natural Resources Research*, vol. 31, no. 1, pp. 261–279, 2022.

[25] B. Li, Z. Shi, Z. Wang, and L. Huang, "Effect of liquid nitrogen freeze–thaw cycles on pore structure development and mechanical properties of coal," *ACS Omega*, vol. 7, no. 6, pp. 5206–5216, 2022.

[26] H. Li, L. Wang, H. Zhang, C. Zhang, H. Zhou, and Y. Geng, "Investigation on damage laws of loading coal samples under cyclic cooling treatment," *Journal of China Coal Society*, vol. 42, no. 9, pp. 2345–2352, 2017.

[27] J. Liu, Y. Xue, Y. Fu, K. Yao, and J. Liu, "Numerical investigation on microwave-thermal recovery of shale gas based on a fully coupled electromagnetic, heat transfer, and multiphase flow model," *Energy*, vol. 263, article 126090, 2023.

[28] E. A. Novikov, V. L. Shkuratnik, and M. G. Zaitsev, "Effect of thermal memory in acoustic emission in fossil coal after predisintegration by cryogenic treatment," *Journal of Mining Science*, vol. 54, no. 6, pp. 883–892, 2018.

[29] V. L. Shkuratnik, S. V. Kuchurin, and V. A. Vinnikov, "Regularities of acoustic emission and thermoemission memory effect in coal specimens under varying thermal conditions," *Journal of Mining Science*, vol. 43, no. 4, pp. 394–403, 2007.

[30] L. Wang, Y. Xue, Z. Cao, X. Wu, F. Dang, and R. Liu, "Mechanical Properties of High-Temperature Granite under Liquid Nitrogen Cooling," *Geofluids*, vol. 2023, Article ID 3819799, 23 pages, 2023.

[31] Y. Chen, L. Tan, N. Xiao, K. Liu, P. Jia, and W. Zhang, "The hydro-mechanical characteristics and micro-structure of loess enhanced by microbially induced carbonate precipitation," *Geomechanics for Energy and the Environment*, article 100469, 2023.